Received: 19 May 2022 | Revised: 1 September 2022 | Accepted: 5 September 2022

IET Science, Measurement & Technology

DOI: 10.1049/smt2.12126

The Institution of Engineering and Technology WILEY

ORIGINAL RESEARCH

Manipulation of stator current signature for rotor asymmetries fault diagnosis of wound rotor induction machine

Mohammad Hoseintabar Marzebali[1] | **Vahid Abolghasemi**[2] | **Saideh Ferdowsi**[2] | **Reza Bazghandi**[1]

[1]Faculty of Electrical Engineering, Shahrood University of Technology, Shahrood, Iran

[2]School of Computer Science and Electronic Engineering (CSEE), University of ESSEX, Colchester, UK

Correspondence
Mohammad Hoseintabar Marzebali, Faculty of Electrical Engineering, Shahrood University of Technology, Shahrood 3619995161, Iran.
Email: m.hoseintabar@shahroodut.ac.ir

Abstract

In this paper, a new technique based on the manipulation of stator current signature for induction machines fault diagnosis is introduced. The goal of the proposed method is to demodulate the characteristic frequencies from supply frequency and preserve the information of the supply frequency and its harmonics. The proposed method can be easily implemented and used in experimental systems due to its low computational complexity. The validity of the proposed method is proved through theoretical analysis and experimental results in steady-state and transient conditions. In this regard, the 270-W wound rotor induction machine (WRIM) is tested under different fault severities and load levels.

1 | INTRODUCTION

Induction machines have been widely used in different applications and are known as key components of industrial systems [1, 2]. Since these machines are faced with different mechanical and electrical faults, condition monitoring of such systems is necessary [3, 4]. A major part of electrical and mechanical faults in induction machines is related to the rotor asymmetries originated from broken rotor bar (BRB) in squirrel cage induction machine or faulty rotor phase in wound rotor induction machine (WRIM) [5, 6].

To ensure safe operation and timely maintenance, different diagnostic methods based on mechanical and electrical signatures have been introduced [7]. Among these, motor current signature analysis (MCSA) has been extensively used for fault detection process due to its non-invasive nature [8].

It has been shown that rotor asymmetries generate fault characteristic frequency ($f_{c,raf}$) around the supply frequency and its harmonics through [1]

$$f_{c,raf} = (1 \pm 2\zeta s) f_1,\ \zeta = 1, 2, 3, \ldots \quad (1)$$

where f_1 and s are supply frequency and slip, respectively. It has been proved that the classical lower ($(1 - 2\ s)f_1$) and upper harmonic ($(1 + 2\ s)f_1$) around the supply frequency have higher amplitudes in comparison with other time and space harmonics. Therefore, $(1 \pm 2\ s)f_1$ are considered dominant fault characteristic frequencies for fault detection in induction machine (IMs) [9]. In this regard, some limitations and constraints such as sideband frequencies detection in light load levels conditions, which can be easily buried by supply frequency, make the utilization of MCSA methods complicated [10, 11]. Moreover, the amplitude of the main characteristic frequency of fault harmonics ($f_{c,raf}$) can be affected by supply frequency or DC component in demodulated signal in the spectrum of current.

Although the presence of supply frequency in the current signature of the stator makes the detection of fault characteristic frequencies complicated, demodulation techniques are effectively utilized to separate these two. Some of the well-known demodulation techniques used in the past are the amplitude of instantaneous stator current space vector (ISCSV) [12, 13], Teager-Kaiser energy operator (TKEO) [14], frequency domain energy operator (FDEO) [15] and square current signal technique. In addition to these methods, BRB fault diagnose based on park vector approach (PVA) is introduced to demodulate the fault characteristic frequency from the supply frequency [13]. As alternative method, the sum of adjacent product (SAP) is introduced for improving fault diagnosis accuracy under large speed variations [16]. Moreover, the sum of squares of stator current is

presented as fault detection methods for BRB in induction IMs [17].

In order to reduce the need for more stator phases, TKEO and FDEO methods are proposed [14, 15]. It should be noted that the main objective of TKEO and FDEO was improving the fault diagnosis, especially in the light loads. However, the amplitude of fault characteristic frequency can be significantly affected by TKEO [10]. Although the TKEO technique has priority in comparison with some conventional methods such as envelope analysis, some limitation such as complexity and incapability to calculate the amplitude of fault characteristic frequency makes TKEO impractical [18, 19]. Demodulation of fault characteristic frequencies through positive and negative sequences of stator current for closed-loop drive systems has been reported in [19]. It seems that [19] cannot be implemented in line-fed induction machines due to asymmetries in the supply frequencies of IMs. An efficient and complex Hilbert-hung demodulated technique has been presented along empirical mode decomposition (EMD) technique to extract fault features from intrinsic mode functions (IMFs) [20]. The analytical signal-based techniques are also used for the demodulation of fault-related frequencies from the main frequency. However, these methods are complex due to Hilbert's transformation (HT) and mathematical computations [20–23]. In other words, the implementation of HT needs two forward FFTs and an inverse FFT which increase the complexity of the methods based on HT. Since TKEO-based methods are sensitive to noise, third-order energy operator (TOEO) technique was introduced for BRB fault in induction machines [24]. Furthermore, TOEO requires minimal calculation in comparison with the TKEO and FDEO techniques. Recently, rectified stator current of IMs has been introduced which is based on the information of single phase of three-phase IMs. The method is simple and can be implemented in real system easily [10].

The amplitudes of fault characteristic frequencies are extremely weak in the incipient stage and light load levels. Consequently, they can be easily buried by the leakage of the supply frequency. Generally, the fast Fourier transform (FFT) technique cannot capture the buried features of a faulty system [11]. As a result, the improvement in the capability of detecting hidden fault characteristic frequencies is of significant interest by researchers in the field. Therefore, demodulated techniques have been proposed. However, these methods generally increase the complexity of the diagnostic system or omit the supply frequency and their harmonics, which changes the nature of the stator current signal. As a result, it will not be possible to analyse the characteristics of the original signal and its harmonics through the new demodulated version.

The main objective of this study is to develop a new method based on the manipulation of stator current signature for rotor asymmetries faults (RAFs) detection. Our simple and yet effective manipulation approach is proposed in time domain, which leads to accurate demodulation of the fault characteristic frequencies, even if it is dominated by the supply frequency. Moreover, the proposed demodulated method can keep the features of supply frequency harmonics and their sidebands. We will mathematically prove that the proposed method can accurately calculate and extract the amplitude of fault characteristic frequencies.

The main contributions of this paper are as follows:

- The proposed method can demodulate the main characteristic frequency component of RAF from the supply frequency to avoid leakage effects.
- Unlike previous methods, the proposed method can preserve the information of the main harmonics in the demodulated signal. The previous methods, such as TKEO [14], NFDEO [15], and rectification of the stator current signal [10], extended park vector [13], and square current signal [17], eliminate the information of the supply frequency and their modulated frequency components. Since the RAF characteristic index in IMs depends on the slip and also the supply frequency, either in the line-fed induction machine or inverter-fed machine, therefore, knowing the exact location of the supply frequency leads to the accurate diagnosis of the RAF in the machine. As a result, slight variations in the supply frequency lead to a change in the place of the RAF index, so many efforts have been made to find the exact place of the supply frequency at any moment by means of the current spectrum. In the previous cases, the frequency place must be measured using the current spectrum at the time of signal measurement, and then that signal is demodulated from the main frequency using the pre-processing method in the next step, while in the proposed method it is possible to identify the supply frequency as well as RAF index in one signal.
- Therefore, preserving the information of both fault and supply frequencies in the proposed method provides a more accurate and reliable fault detection result in comparison with the previous methods.
- The proposed method, unlike some previous methods such as the instantaneous amplitude of the stator current space vector and phase, needs only the information of single phase of three-phase machine [2, 25].
- The method has clear mathematical derivation and can be inexpensively implemented for fault detection in IMs with simple software algorithm.

The rest of this paper is organized as follows. In the next section, the mathematical description of fault characteristic harmonics modulation in the presence of supply frequency is given. In Section 3, the comparison between demodulation techniques for electrical signature analysis is presented. The proposed technique is introduced in Section 4. Test-rig description and experimental results are given in Sections 5 and 6, respectively. Finally, the paper is concluded in Section 7.

2 | FAULT HARMONICS IN THE STATOR CURRENT SIGNATURE OF INDUCTION MACHINE WITH ROTOR ASYMMETRIES

Fault characteristic frequencies occurred through asymmetries in the rotor of an induction machine (1) can be simply described

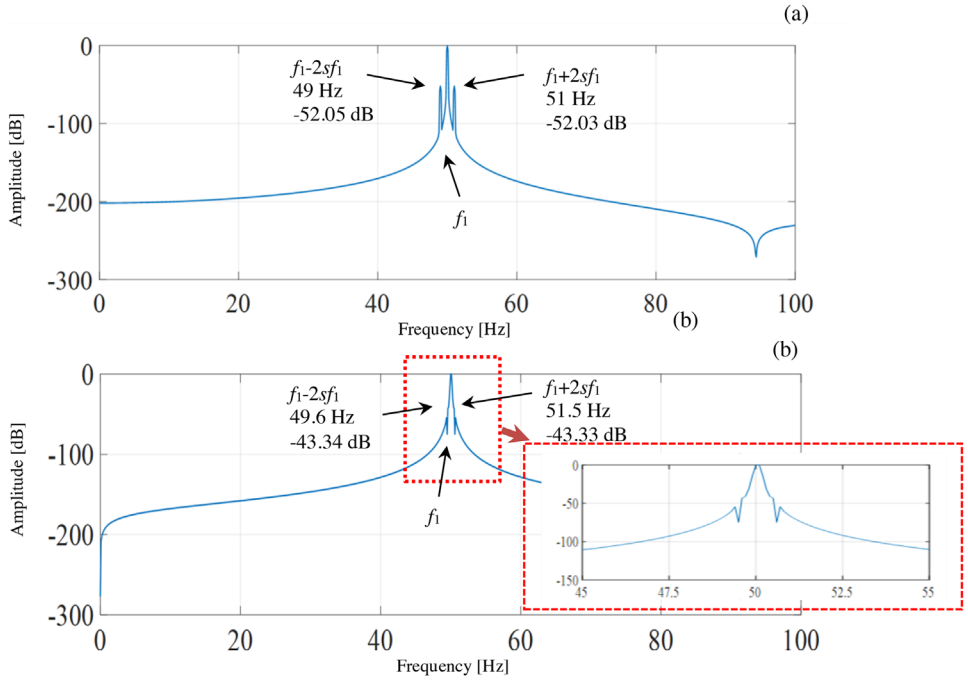

FIGURE 1 (a) Spectrum of $i_N(t)$ with $s = 0.01, f_1 = 50, \gamma = 0.005$. (b) Spectrum of $i_N(t)$ with $s = 0.005, f_1 = 50.05, \gamma = 0.005$

in the stator current of IMs as (2) [10].

$$i(t) = \sum_{b=1,3,5,\ldots} I_b \cos(2\pi b f_1 t)(1 + \gamma \cos(2\pi(2ksf_1)t), \quad (2)$$

where I_1, f_1, and γ are maximum amplitude of stator current, supply frequency and severity of the fault, respectively. Simplification of (2) with neglecting the effects of other harmonics of supply frequency and RAF shows that the stator current spectrum has three components including supply

frequency (f_1) and two modulated sidebands frequencies of fault ($f_1 \pm 2sf_1$):

$$\begin{aligned} i(t) &= I_1 \cos(2\pi f_1 t) + \frac{\gamma}{2} I_1 \cos(2\pi(1-2s) f_1 t) \\ &+ \frac{\gamma}{2} I_1 \cos(2\pi(1+2s) f_1 t), \end{aligned} \quad (3)$$

As observed from (3), the presence of the fault in IMs leads to additive frequencies around the supply frequency ($f_1 \pm 2ksf_1$) [10]. Taking Fourier transform (FT) of normalized $i(t)$, that is, $i_N(t) = (i(t))/I$, leads to

$$FT\{i_N(t)\} = 1 \times \delta(f - f_1) + \frac{\gamma}{2} \times \delta(f - (f_1 \pm 2sf_1)), \quad (4)$$

Fault characteristics frequency in (4) has $\gamma/2$ amplitude, which is equivalent to $20 \times \log(\gamma/2)$ dB, when converted to the logarithmic domain. This can be seen from Figure 1a where the spectrum of $i_N(t)$ in two different conditions is depicted.

It can be also found that the leakage of supply frequency affects the detection of fault characteristic frequency especially in the light load level or low slips (Figure 1b). Figure 1 shows that as slip decreases, under similar fault severity ($\gamma = 0.005$), the leakage of supply frequency causes inaccurate fault severity values (look at −43.34 dB in Figure 1b compared to −54.05 dB when $s = 0.005$). Therefore, different demodulation techniques have been introduced [10]. In this regard, four popular methods including rectified stator current, a square current signal, the amplitude of analytical signal, and Teager–Kaiser have been used as demodulation techniques for the detection of fault severity. Figure 2 shows that the demodulated fault characteristic frequency emerges near the DC component ($2sf_1$). It is shown in Figure 1b that due to leakage effects, the characteristic frequency of fault cannot be detected in the

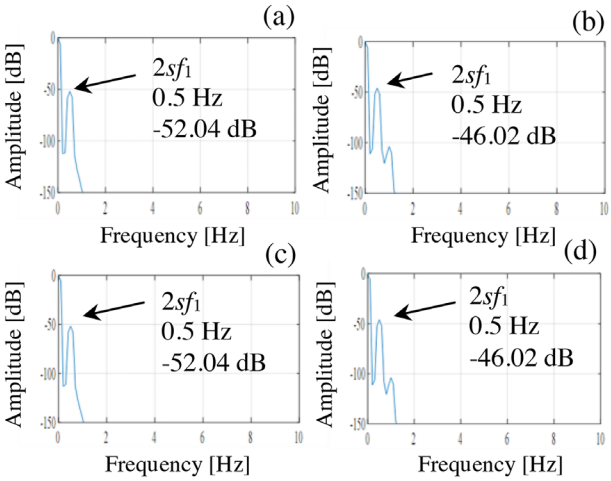

FIGURE 2 (a) Spectrum of stator current with $s = 0.005, f_1 = 50.05, \gamma = 0.005$. (a) Rectified stator current, (b) square current signal, (c) analytic signal, (d) Teager–Kaiser method

TABLE 1 Comparison between different demodulation techniques for electrical signatures analysis

Method	Required number of phases	Formulation	Amplitude of fault based on normalized FFT (dB)	Keeping the features of supply frequency and their harmonics
Analytic signal	1	$i(t)+j.HT\{i(t)\}$	$20\log(\gamma/2)$	×
Extended park vector approach	3	$i_D(t) + j\cdot i_Q(t)$	$20\log(\gamma/2)$	×
Teager–Kaiser energy operator	1	$i^2(t)-i(t)\cdot i''(t)$	$20\log((4+s^2)\gamma/2)$	×
Square current signal	1	$i^2(t)$	$20\log(\beta/(1+2\gamma^2))$	×
Rectified stator current	1	$Abs\{i(t)\}$	$20\log(\gamma/2)$	×
Frequency domain energy operator	1	$i'^2(t)+(HT\{i'(t)\})^2$	$20\log((4+s^2)\gamma/2)$	×

spectrum of stator current signature. However, the fault index can be detected through demodulation techniques where the dominant frequency transforms to the DC frequency (Figure 2 (. This allows us to easily remove the DC component with significantly reduced leakage effects from the fundamental component leading to improved accuracy of the diagnostic procedure.

3 | METHODS

In this section, different demodulation techniques, previously used for the separation of fault characteristic frequency and supply frequency, are compared. In this regard, the relevant studies listed in Table 1 will be reviewed. The best method based on indices of simplicity, the accuracy of fault amplitude, and the number of current sensors is introduced. Then, the drawbacks of the selected method are explained (Table 1). Finally, the mathematical definition of the proposed technique is described. It is shown that the proposed approach mitigates the drawbacks of related works.

3.1 | Comparison of demodulation techniques

Comparison between different demodulation techniques, presented recently, has been carried out in Table 1. In this regard, analytical signal [10], extended park approach [13], TEKO [14], a square current signal, rectified signal [10], and FDEO [15] are compared in the terms of the required number of phases and amplitude of fault.

It can be found from Table 1 that the rectified stator current signature has remarkable priority in fault detection process in comparison to other methods. This method has three important characteristics including one-phase data, simplicity, and accuracy in the computation of fault amplitude. The rectified stator current can be easily implemented in the experimental system. However, all the reviewed methods cannot be able to keep the information of supply frequency, and their harmonics. Generally, some methods such as extended park vectors, TKEO, and rectified signal omit the supply frequency and its harmonics in the demodulated signal. Therefore, the remaining information of the demodulated signal is limited to some sidebands.

3.2 | Mathematical definition of the proposed technique

The main feature of our proposed method is mitigating drawbacks of the previous methods as well as preserving their advantages. Our goal in this method is to demodulate the fault characteristic from the main frequency as accurately as possible. Moreover, the proposed technique can keep the information of supply frequency and their harmonics in the spectrum of demodulated signal through manipulation of given data. To do this, a squared waveform denoted by $g(t)$ is introduced and then multiplied to the original signal $i(t)$ (also depicted in Figure 3).

$$g(t) = \begin{cases} 1, & i(t) > 0 \\ k, & i(t) <= 0 \end{cases} \tag{5}$$

$$i_{N\_m}(t) = i_m(t) \times g(t), \tag{6}$$

where $i_m(t)$ denotes the original current signal, and $i_{N\text{-}m}(t)$ is modulated signal corresponding to $i_m(t)$ (using the squared wave). If $k = -1$, the modified signal (i.e. $i_{N\text{-}m}(t)$) is converted into the rectified signal. As can be observed from (5) and Figure 3, $g(t)$ converts the original signal ($i_m(t)$) to the new modulated signal through the multiplication process in the time domain. To demonstrate how the proposed manipulation in time domain can facilitate fault diagnosis in the frequency domain, we first expand $g(t)$ and $i_{N\text{-}m}(t)$ via (7) and (8), respectively.

$$g(t) = \frac{k+1}{2} + \sum_{n=1}^{n=\infty} \frac{2}{\pi n}[(1-k)\sin(\frac{n\pi}{2})]\cos(n2\pi f_1 t) \tag{7}$$

$$\begin{aligned} i_{N-m}(t) = {} & \frac{k+1}{2}\left[\begin{array}{l}\sum_{h=1}^{\infty} I_h \cos(h(2\pi f_1)t)+ \\ +\frac{\gamma}{2} I_h \cos(h(2\pi f_1)(1\pm 2s)t)\end{array}\right]+ \\ & + \left[\sum_{n=1}^{n=\infty} \frac{2}{\pi n}[(1-k)\sin(\frac{n\pi}{2})]\cos(n2\pi f_1 t)\right]\times \\ & \times \left[\sum_{h=1}^{\infty} I_h \cos(h(2\pi f_1)t) + \frac{\gamma}{2} I_h \cos(h(2\pi f_1)(1\pm 2s)t)\right] \end{aligned} \tag{8}$$

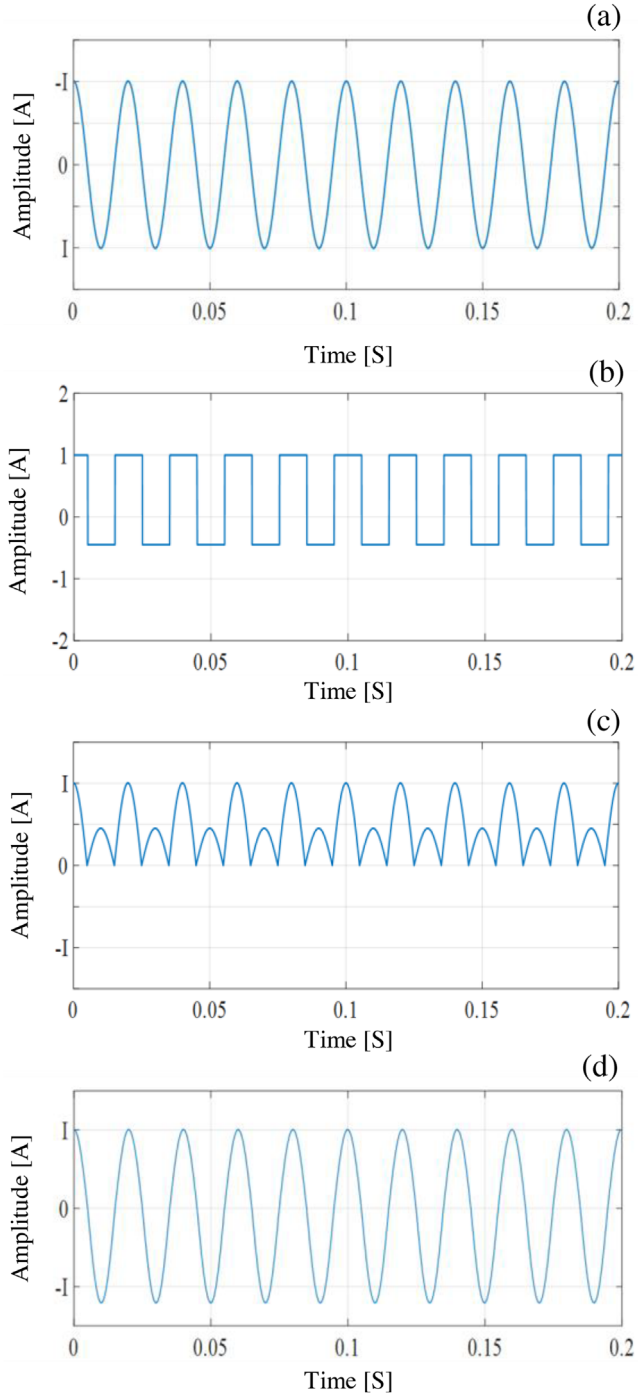

FIGURE 3 (a) Original signal of $i_N(t)$ with $s = 0.005, f_1 = 50.05, \gamma = 0.005$, (b) $g(t)$, (c) i_{N_m} for $k = -0.2$, (d) i_{N_m} for $k = 1.2$

Then, their corresponding FT is given in (9).

$$FT\{i_N(t)\}(f) = |i_N|(f) = \left|\frac{1}{2}I_1\frac{(2-2k)}{\pi}\right|\delta(f) + \left|\frac{1}{2}I_1\frac{1}{\pi}(2-2k)\frac{\gamma}{2}\right|\delta(f-2sf_1) + \left|\frac{1}{2}\frac{k+1}{2}I_1\right|\delta(f-f_1) + \left|\frac{1}{2}\frac{k+1}{2}\frac{\gamma}{2}I_1\right|\delta(f-(f_1\pm 2sf_1)) + \cdots, \quad (9)$$

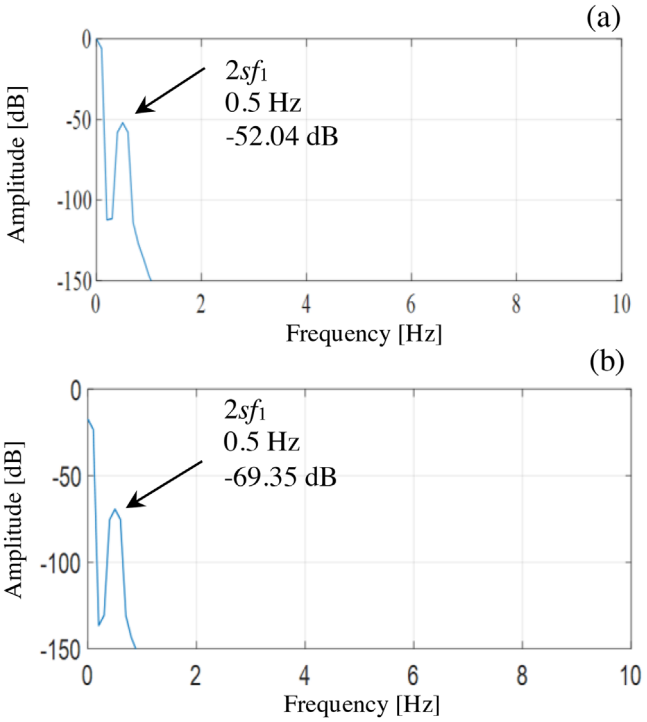

FIGURE 4 Fourier transform of machine stator current signal with $s = 0.005, f_1 = 50.05, \gamma = 0.005$. (a) $k = -0.2$, (b) $k = 1.2$

The result of expansion based on FT shows that the fault characteristic frequency is demodulated from the main frequency while the main harmonic of supply frequency exists in the spectrum of stator current (9). It is worth mentioning that even with $k = 0$, which is equivalent to half-cycle rectification, the same conclusion can be made. In other words, replacing some data points with zero can also demodulate the fault characteristic frequency from the main frequency. It is necessary to note that the normalization of fault amplitude to the DC value $(0.5 \times I_1 \times (2 - 2k)/\pi)$ in the spectrum of stator current leads to the independence of fault characteristic frequency from k (10). As a result, inspecting the spectrum of stator current signatures for two different k values (e.g. $k = -0.2$ and $k = 1.2$) shows that demodulated fault characteristic frequency $(2sf_1)$ with the proposed technique has accurate and the same amplitudes (Figure 4).

In Figure 5, the proposed method is compared from the viewpoint of the presence of main frequency harmonics. In this regard, the main harmonic, along with its third harmonic, is taken into consideration. Among various reviewed methods, the signal rectification method, which is the simplest method of demodulating the sideband frequencies, is considered for the comparison process. The results show that based on (8) unlike previous methods, the proposed method can maintain the dominant frequency and its harmonics in the spectrum of the proposed demodulated technique (Figure 5).

Since the proposed method converts the fundamental component into a DC component (corresponding to zero frequency) the frequency leakage (due to signal truncation in time domain) is minimized. This is because a DC signal can be

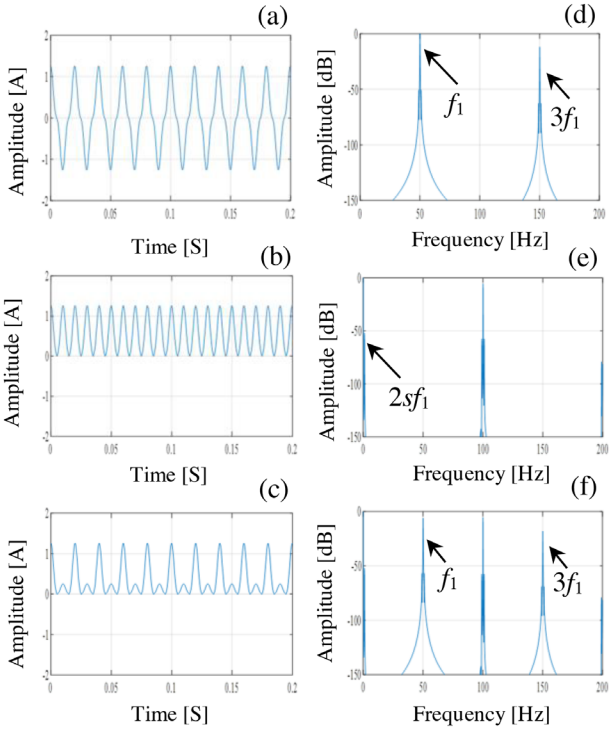

FIGURE 5 (a) Original signal of i_N (t) with $s = 0.005, f_1 = 50.05$, $\gamma = 0.005$, $I_1 = 1$, and $I_3 = 0.25$. (b) Rectified of original signal. (c) i_{N_m} for $k = -0.2$. (d) Spectrum of original signal. (e) Spectrum of rectified of original signal. (f) Spectrum of i_{N_m} for $k = -0.2$

truncated at any location and at any length, without concerning about period boundaries, which is one of the main reasons of occurring frequency leakage in the Fourier spectrum. This approach allows detection of fault harmonics with very small amplitude which could be buried under the leakage of the fundamental component in the original spectrum.

In fact, there are other methodologies aiming to perform such transformation but using different approaches, for example, by analysing the spectrum of the current envelope (which can somehow resemble the DC component) [26–28]. However, the proposed method in this study is a more accurate, straightforward, and less expensive to convert the fundamental component into a DC component.

$$\left|i_f\right|_{dB} = 20\log(\frac{\gamma}{2}), \tag{10}$$

4 | EXPERIMENTAL RESULTS

In this section, the structure of the experimental system implemented for the evaluation of the proposed method is described. For this purpose, a 270-W WRIM with available rotor terminals which have a nominal voltage of 400 V, four poles, and a rated speed of 1370 rpm is used for the fault detection process.

This machine is controlled through a digital brake system. To emulate the asymmetries faults, external resistance with different values is added to the rotor circuit of the machine (R_{unb}).

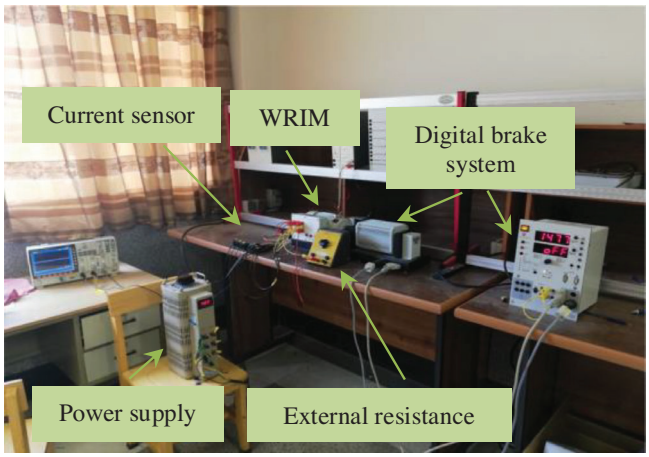

FIGURE 6 Test-rig system description for analysis of asymmetries in the rotor circuit of IMs. IMs, induction machine.

The measured stator current is used for the fault detection process. Figure 6 shows the test-rig of the experimental system. In this regard, the stator current of WRIM in healthy and three faulty cases has been measured to investigate the effects of faults on the characteristic frequency in different fault severities. As observed from Figure 7, as the fault severity increases, the amplitude of characteristic frequency grows. The spectra of stator current show that the fault characteristic frequency emerges as additive frequencies around the main frequency.

4.1 | Steady-state conditions

It is worth noting that the fault characteristic frequency gets closer to the supply frequency as the slip decreases. Since the supply frequency is dominant, the fault detection process becomes challenging due to significant leakage effects. In the proposed method, the supply frequency is preserved through the entire fault detection procedure. Since the amplitude of the DC component and main harmonic change with the variations of k, the normalized fault characteristic frequency with considering the maximum value of dominant frequency, which can be DC component or supply frequency, has an inaccurate value and may be related to the value of k. As it was mathematically shown above, in cases where the supply frequency is dominant, the normalized fault characteristic frequency based on (9) would be related to the k ($[2(1-k)\gamma/(\pi(1+k))]$). However, in cases where the DC component is detected as dominant frequency, the ratio of the normalized fault characteristic frequency to the maximum value of frequency components would be independent of the value of k and has its accurate value ($20\log(\gamma/2)$). It has been proved in mathematical analysis that for any value of k, the ratio of the normalized value of fault characteristic frequency to the DC component is independent of k ($20\log(\gamma/2)$).

For this purpose, the relationship between supply frequency and the DC component to the k factor has been given in (11).

$$|k+1|\frac{I_1}{4} < |1-k|\frac{I_1}{\pi} \Rightarrow k < \frac{4-\pi}{4+\pi}, k > \frac{4+\pi}{4-\pi} \tag{11}$$

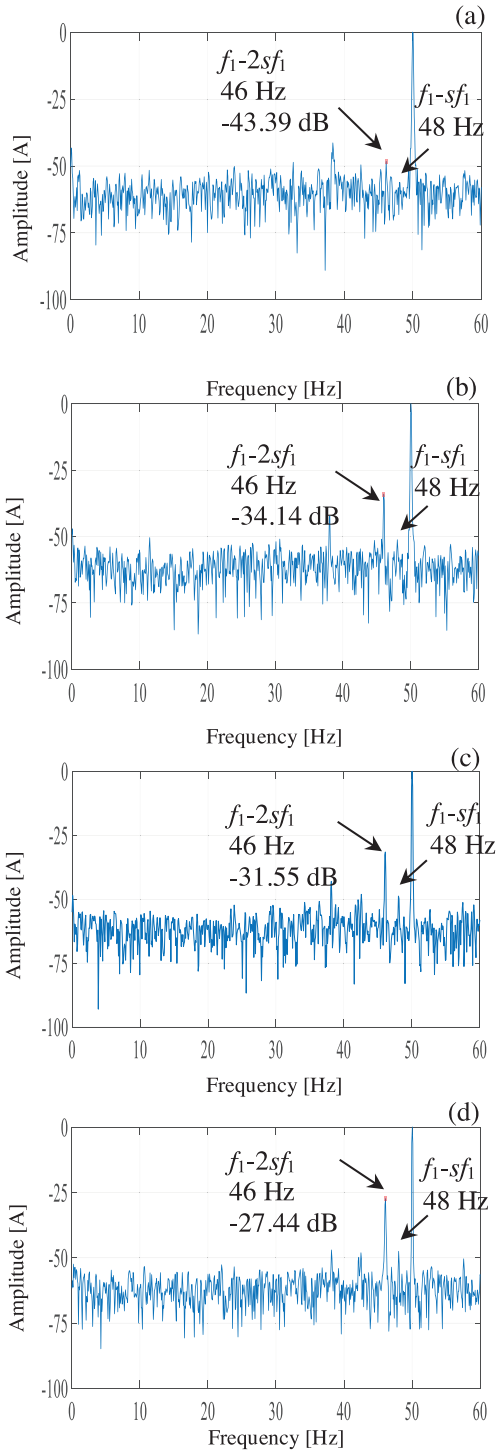

FIGURE 7 Experimental results of stator current spectra with $s = 0.04$. (a) Healthy, (b) $R_{unb} = 0.029$ p.u., (c) $R_{unb} = 0.059$ p.u., (d) $R_{unb} = 0.088$ p.u.

The normalization process in experiments in case where the DC component has less amplitude in comparison with supply frequency may lead to an increase in the noise level of the current spectrum. Consequently, the appropriate range for the case of the DC harmonic, which has a higher value of frequency component in comparison with supply frequency, needs to be calculated.

Suppose that the white noise in the spectrum of the stator current can be written as (12).

$$P = \sum_{n=0}^{n=\infty} P_0 \cos(n(\Delta\omega)t + \varphi_n), \tag{12}$$

The amplitude of noise level ($P_N(f)$) in the spectrum of stator current can be calculated in the two ranges of k factor as they are given in (13).

$$\begin{aligned} P_N(f) &= 20\log\left(\frac{2|P_0|}{|I_1|}\right), if \frac{4-\pi}{4+\pi} < k < \frac{4+\pi}{4-\pi} \\ P_N(f) &= 20\log\left(\frac{2|P_0|\left|\frac{k+1}{4}\right|}{|I_1|\left|\frac{1-k}{\pi}\right|}\right), if k < \frac{4-\pi}{4+\pi}, k > \frac{4+\pi}{4-\pi} \end{aligned} \tag{13}$$

In order to keep the amplitude of RAF characteristic frequency at $20 \times \log(\gamma/2)$, the range of k factor needs to be set at $(k < \frac{4-\pi}{4+\pi}, k > \frac{4+\pi}{4-\pi})$. In this regard, the noise level is smaller in comparison with k factor at the range of $(\frac{4-\pi}{4+\pi} < k < \frac{4+\pi}{4-\pi})$. This is obtained due to the fact that for $\{k < \frac{4-\pi}{4+\pi}, k > \frac{4+\pi}{4-\pi}\}$ to be valid, the term $|k+1|\frac{I_1}{4} < |1-k|\frac{I_1}{\pi}$ needs to be met (Figure 8).

The appropriate range in which the DC component would be higher than supply frequency is calculated and represented $(k > ((4+\pi)/(4-\pi))$ and $k < ((4-\pi)/(4+\pi)))$ (11). It is necessary to note that the selection of k by operator out of allowable range leads to an increase in the noise level (more than 50 dB, Figure 9c). Therefore, the fault characteristic cannot be calculated correctly. To assess the performance of the proposed technique for fault detection in IMs, different values of k are considered and stator current spectrum is given for the different values of k in Figure 9. To verify the results of the proposed technique with previous related methods, rectified stator current which can be obtained by $k = -1$ is considered. The fault characteristic frequency is demodulated from supply frequency (Figure 9). However, as seen from Figure 9c, for $k = 1.2$ which is out of the allowable range ($k > 8.32$ and $k < 0.12$) (Figure 7), the amplitude of fault characteristic frequency cannot be detected. It is worth mentioning that the amplitude of fault characteristic frequency does not significantly change with variations of k. It approximately remains constant, which is an indication that the fault characteristic frequency is independent of k (Figure 9).

The fault characteristic frequencies for fault detection in IMs due to RAFs are related to $(f_1 \pm 2sf_1)$. It has been shown that the classical lower $((1-2s)f_1)$ and upper harmonic $((1+2s)f_1)$ around the supply frequency have higher amplitudes in comparison with other time and space harmonics. Therefore, $((1+2s)f_1$ are considered dominant fault characteristic frequencies for fault detection in IMs. Therefore, in this paper, the mentioned RAF characteristic frequency is considered for the detection of fault and other frequencies which are affected by interaction between harmonics or noises are not investigated.

Through all the simulation and experimental results, we have used the Hanning window to provide a good frequency res-

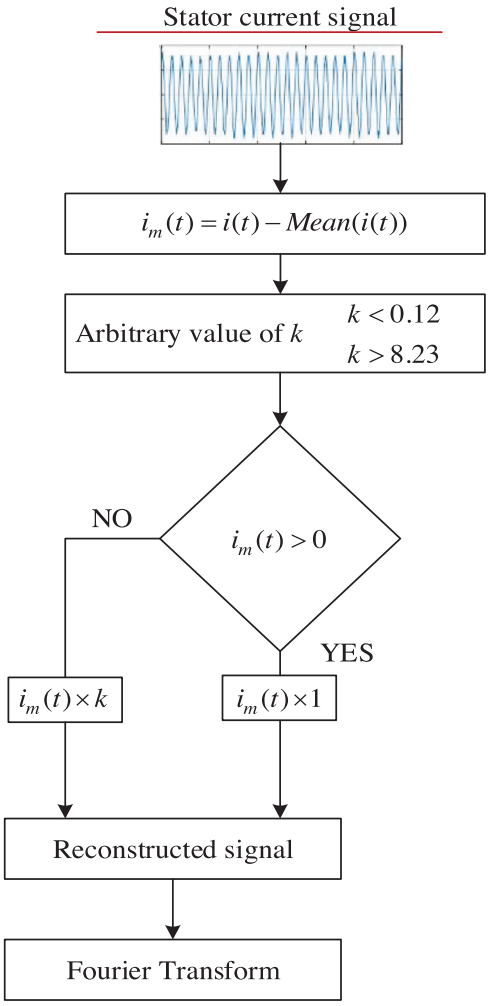

FIGURE 8 Flowchart of proposed demodulated technique

olution and reduce the leakage effect with a fair amplitude accuracy. This procedure was applied to both modulated and non-modulated signals. It is observed from the obtained results that the demodulation using the proposed method provides a better frequency distinction compared to the no demodulation case while a Hanning window is used.

4.2 | Transient conditions

The performance of the proposed method in transient conditions (dynamic speed) has been evaluated under two acceleration and deceleration modes. Generally, the methods presented have been analysed based on the use of current signal in the start-up mode of the machine. However, in order to emulate the dynamic behaviour of IMs in transient conditions, the speed of the studied machine has been changed slightly in the acceleration and deceleration modes.

In acceleration mode, the speed of IMs has been changed from 1400 to 1450 rpm (Figure 10a). The time–frequency spectrum of stator current signal using the Fourier synchro-squeezed transform (FSST) method is shown in Figure 10b in which the

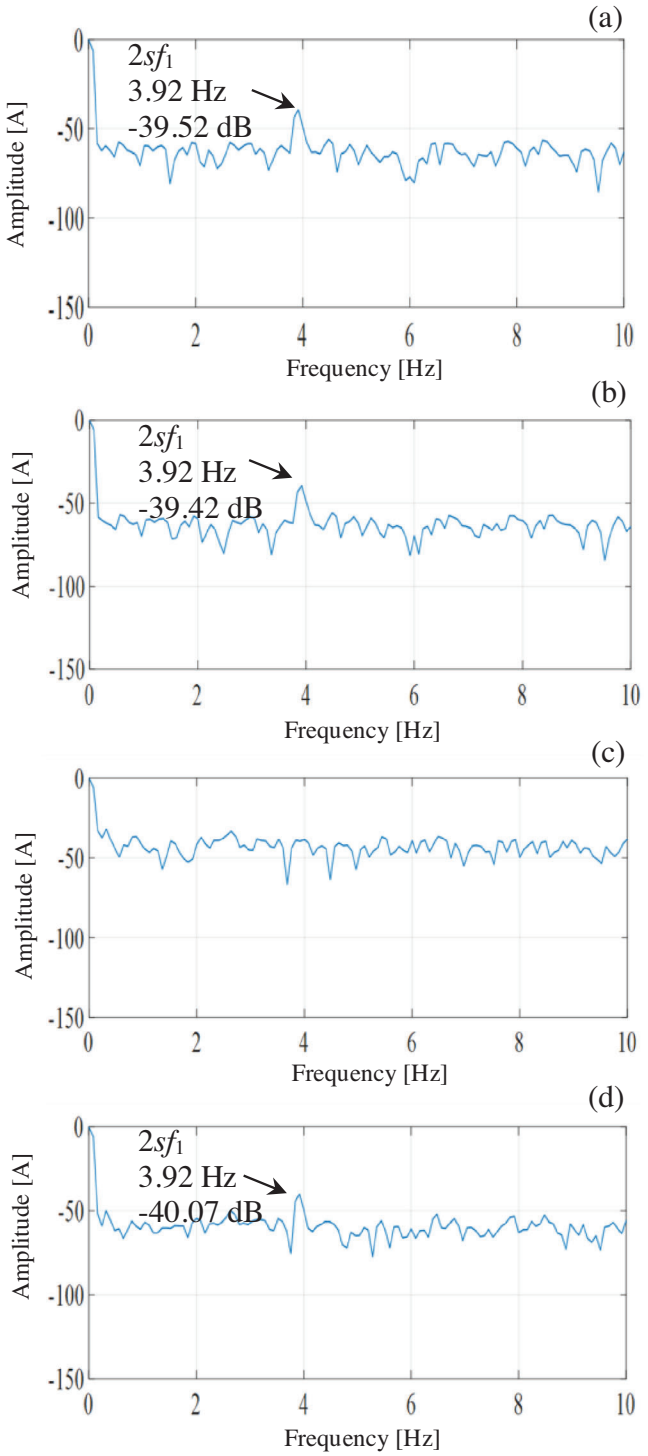

FIGURE 9 Experimental results of stator current spectra by demodulated proposed technique with $s = 0.04$ and $R_{unb} = 0.059$ p.u. (a) $k = -1.5$, (b) $k = -1$, (c) $k = 1.2$, (d) $k = 10$

RAF index is well visible in the vicinity of the supply frequency (50 Hz). The RAF index gets closer to the frequency of the power supply by increasing the speed, so it will be difficult to detect the index at no-load speed or low slips.

The proposed method is evaluated in four values of k in transient mode. In $k = -1$, the RAF index is demodulated

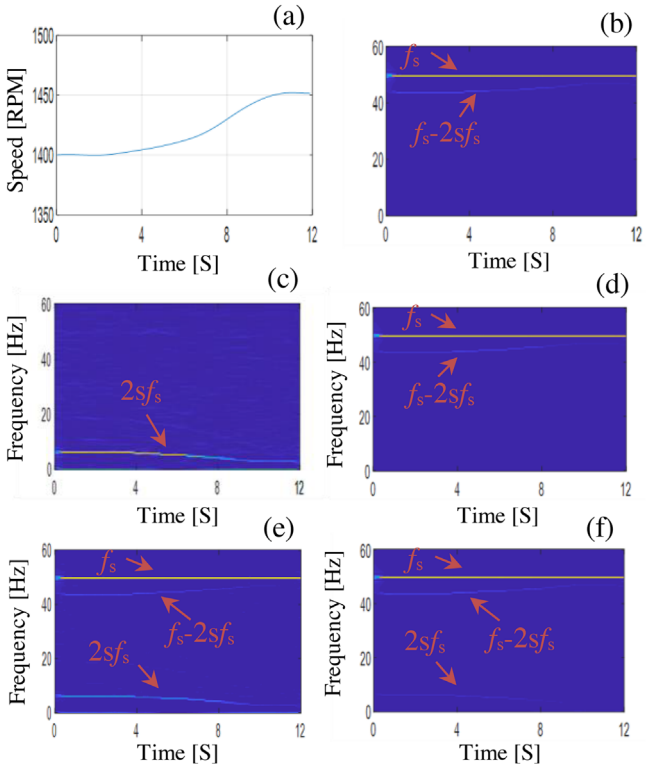

FIGURE 10 Experimental results of stator current spectra by demodulated proposed technique in transient condition and R_{unb} = 0.059 p.u. (a) Speed, (b) FSST of stator current at stator current, (c) FSST of stator current at $k = -1$, (d) FSST of stator current at $k = 1.2$, (e) FSST of stator current at $k = -1.5$, (f) FSST of stator current at $k = 10$. FSST, Fourier synchro-squeezed transform.

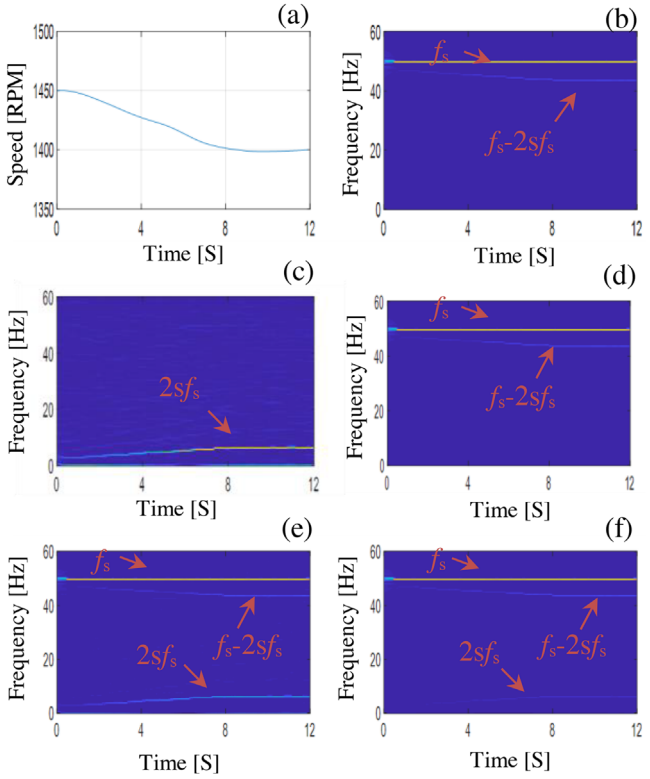

FIGURE 11 Experimental results of stator current spectra by demodulated proposed technique in transient condition and R_{unb} = 0.059 p.u. (a) Speed, (b) FSST of stator current, (c) FSST of stator current at $k = -1$, (d) FSST of stator current at $k = 1.2$, (e) FSST of stator current at $k = -1.5$, (f) FSST of stator current at $k = 10$

from the main frequency and will be visible near the zero frequency. In this case the supply frequency has been eliminated (Figure 10c). In $k = 1.2$ which is not within the permissible range, the RAF index is not visible close to the zero frequency as it has been expected (Figure 11d). In $k = 10$, RAF index similar to $k = -1.5$. The RAF index is demodulated and can be detected close to the zero frequency. Furthermore, the supply frequency also can be observed (Figures 10e and 10f).

In deceleration mode, the speed of IMs has been changed from 1450 to 1400 rpm (Figure 11a). The time–frequency spectrum of the stator current signal using the FSST method is shown in Figure 11b in which the RAF index is well visible in the vicinity of the supply frequency (50 Hz). The RAF index gets closer to the frequency of the power supply by decreasing the speed, so it will be difficult to detect the index at no-load speed or low slips.

Similar to the acceleration mode, the proposed method is evaluated under four values of k in deceleration mode. In $k = -1$, the RAF index is demodulated from the main frequency and will be visible near the zero frequency. In this case the supply frequency has been eliminated (Figure 11c). In $k = 1.2$ which is not within the permissible range, the RAF index is not visible close to the zero frequency as it has been expected (Figure 11d). In $k = 10$, the RAF index is similar to that in $k = -1.5$. The RAF index is demodulated and can be detected close to the zero frequency. Furthermore, the supply frequency can also be observed (Figures 11e and 11f).

5 | CONCLUSION

In this paper, a generalized method based on the manipulation of stator current signature for RAF detection in the stator current signatures of IMs is proposed. The main concept of the presented method is based on the multiplication of the original signal by the function which includes the dominant frequency of the original signal. The performance of the proposed technique is verified through experiments and can be easily used for the demodulation of RAF from the main frequency. One of the main advantages of the proposed method is that it can simply be implemented in the experimental system and unlike previous demodulated techniques maintain the dominant frequency and their harmonics in the spectrum of demodulated proposed stator current.

AUTHOR CONTRIBUTION

Mohammad Hoseintabar Marzebali: Conceptualization, Formal analysis, Methodology, Writing – original draft

Vahid Abolghasemi: Data curation, Formal analysis, Methodology, Writing – original draft, Writing – review & editing

Saideh Ferdowsi: Formal analysis, Investigation, Validation, Writing – review & editing

Reza Bazghandi: Investigation, Validation, Writing – review & editing

CONFLICT OF INTEREST

We have no conflict of interest to declare.

FUNDING INFORMATION

This research received no specific grant from any funding agency in the public, commercial, or not-for-profit sectors.

DATA AVAILABILITY STATEMENT

The data that support the findings of this study are available from the corresponding author upon reasonable request.

REFERENCES

1. Marzebali, M.H., et al.: Planetary gearbox torsional vibration effects on wound-rotor induction generator electrical signatures. IEEE Trans. Industry Appl. 52(6), 4770–4780 (2016)
2. Marzebali, M.H., et al.: Planetary gear fault detection based on mechanical torque and stator current signatures of a wound rotor induction generator. . IEEE Trans. Energy Convers. 33(3), 1072–1085 (2018)
3. Abolghasemi, V., Marzebali, M.H., Ferdowsi, S.: Recursive singular analysis for induction machines unbalanced rotor fault diagnosis. IEEE Trans. Instrum. Meas. 71, 1–11 (2021)
4. Liu Y., Bazzi, A.M.: A review and comparison of fault detection and diagnosis methods for squirrel-cage induction motors: State of the art. ISA Trans. 70, 400–409 (2017)
5. Liu Z., Zhang, L.: A review of failure modes, condition monitoring and fault diagnosis methods for large-scale wind turbine bearings. Measurement 149, 107002 (2020)
6. Kim, H., Lee, S.B., Park, S.: Reliable detection of rotor faults under the influence of low-frequency load torque oscillations for applications with speed reduction couplings. IEEE Trans. Ind. Appl. 52(2), 1460–1468 (2015)
7. Kumar, S., et al.: A comprehensive review of condition based prognostic maintenance (CBPM) for induction motor. IEEE Access 7, 90690–90704, (2019)
8. Gritli, Y., et al.: Advanced diagnosis of electrical faults in wound-rotor induction machines. IEEE Trans. Ind. Electron. 60, 4012–4024 (2013)
9. Henao, H., Razik , H., Capolino, G.-A.: Analytical approach of the stator current frequency harmonics computation for detection of induction machine rotor faults. IEEE Trans. Ind. Appl. 41(3), 801–807 (2005)
10. Puche-Panadero, R., et al.: Diagnosis of rotor asymmetries faults in induction machines using the rectified stator current. IEEE Trans. Energy Convers. 35(1), 213–221 (2019)
11. Puche-Panadero R., et al.: New method for spectral leakage reduction in the FFT of stator currents: Application to the diagnosis of bar breakages in cage motors working at very low slip. IEEE Trans. Instrum. Meas. 70, 1–11 (2021)
12. Kia, S.H., Hajjaji, A.E., Marzebali, M.H.: Planetary gear tooth fault detection using stator current space vector analysis in induction machine-based systems. In: 2019 23rd International Conference on Mechatronics Technology (ICMT), pp. 1–6 (2019)
13. Gyftakis, K.N., et al.: Introducing the filtered Park's and filtered extended Park's vector approach to detect broken rotor bars in induction motors independently from the rotor slots number. Mech. Syst. Signal Process. 93, 30–50 (2017)
14. Pineda-Sanchez M., et al.: Application of the Teager–Kaiser energy operator to the fault diagnosis of induction motors. IEEE Trans. Energy Convers. 28(4), 1036–1044 (2013)
15. Li, H., et al.: A normalized frequency-domain energy operator for broken rotor bar fault diagnosis. IEEE Trans. Instrum. Meas. 70, 1–10 (2021)
16. Cruz S., Cardoso A.: Rotor cage fault diagnosis in three-phase induction motors by extended park's vector approach. Electric Mach. Power Syst. 28(4), 289–299 (2000)
17. Garcia-Calva, T.A., et al.: Demodulation technique for broken rotor bar detection in inverter-fed induction motor under non-stationary conditions. IEEE Trans. Energy Convers. 34(3), 1496–1503 (2019)
18. Li, H., et al.: Modulation sideband separation using the Teager–Kaiser energy operator for rotor fault diagnostics of induction motors. Energies 12(23), 44–37 (2019)
19. Guellout, O., et al.: Elimination of broken rotor bars false indications in induction machines. Math. Comput. Simul. 167, 250–266 (2020)
20. Elbouchikhi, E., et al.: An efficient Hilbert–Huang transform-based bearing faults detection in induction machines. IEEE Trans. Energy Convers. 32(2), 401–413 (2017)
21. Abd-el, M., Abdelsalam, A.K., Hassan, O.E.: Induction motor broken rotor bar fault location detection through envelope analysis of start-up current using Hilbert transform. Mech. Syst. Signal Process. 93, 332–350 (2017)
22. Abd-el, M.B., Abdelsalam, A.K., Hassan, O.E.: Novel approach using Hilbert Transform for multiple broken rotor bars fault location detection for three phase induction motor. ISA Trans. 80, 439–457(2018)
23. Matić, D., et al.: Support vector machine classifier for diagnosis in electrical machines: Application to broken bar. Expert Syst. Appl. 39(10), 8681–8689 (2012)
24. Wang W., et al.: Induction motor broken rotor bar fault diagnosis based on third-order energy operator demodulated current signal. IEEE Trans. Energy Convers. 37(2), 1052–1059 (2022). https://doi.org/10.1109/TEC.2021.3121788
25. Kia S.H., Henao H., Capolino G.-A.: Gear tooth surface damage fault detection using induction machine stator current space vector analysis. IEEE Trans. Ind. Electron. 62(3), 1866–1878 (2015). https://doi.org/10.1109/TIE.2014.2360068
26. Cheng F., et al.: Fault diagnosis of wind turbine gearboxes based on DFIG stator current envelope analysis. IEEE Trans. Sustain. Energy 10(3), 1044–1053 (2018)
27. Xu B., et al.: Improvement of the Hilbert Method via ESPRIT for detecting rotor fault in induction motors at low slip. IEEE Trans. Energy Convers. 28(1), 225–233 (2013)
28. Puche-Panadero R., et al.: Improved resolution of the MCSA method via Hilbert transform, enabling the diagnosis of rotor asymmetries at very low slip. IEEE Trans. Energy Convers. 24(1), 52–59 (2009)

How to cite this article: Marzebali, M.H., Abolghasemi, V., Ferdowsi, S., Bazghandi, R.: Manipulation of stator current signature for rotor asymmetries fault diagnosis of wound rotor induction machine. IET Sci. Meas. Technol. 16, 523–532 (2022). https://doi.org/10.1049/smt2.12126